Journal of Applied Research and Technology

www.jart.icat.unam.mx

Journal of Applied Research and Technology 21 (2023) 796-807

Original

Application of porous geopolymer composite 1 based on metakaolin and activated 2 carbon for removal of Hg^2+ from aqueous solution

K. Roa[a,b*] • F. Trejo[a] • H. Castro[b]

[a]*Center for Research in Applied Science and Advanced Technology (CICATA), National Polytechnic Institute, Mexico City, Mexico*
[b]*Pedagogical and Technological University of Colombia, Sogamoso, Colombia*

Received 07 09 2021; accepted 04 10 2023
Available 10 31 2023

Abstract: This paper reviews the application of a geopolymer composite using an easy synthesis route based on the activation of metakaolin (MK) as aluminosilicate source and activated carbon (AC) as a porous agent, to improve porosity and adsorption capacity. The main goal of this study is to evaluate the ability of the obtained geopolymer to remove Hg^{2+} from aqueous solutions, for comparison purposes a geopolymer sample was fully synthesized with metakaolin aluminosilicates. The samples were investigated by X-ray fluorescence (XRF), Fourier transform infrared spectroscopy (FTIR), compressive strength tests, and scanning electron microscopy (SEM). Hg^{2+} removal from aqueous solutions was quantified using inductively coupled plasma optical emission spectroscopy (ICP-OES). The pH of the solution significantly affects the adsorption of Hg^{2+} ions onto the geopolymer surface. The maximum removal efficiency of the composite was 87.6 % at room temperature and pH 5. These results suggest the use of a geopolymer with activated carbon as a successful alternative adsorbent for Hg^{2+} ions in water.

Keywords: Geopolymer, activated carbon, alkali activation, mercury, adsorption

*Corresponding author.
E-mail address: karol.roa@uptc.edu.co (K. Roa).
Peer Review under the responsibility of Universidad Nacional Autónoma de México.

1. Introduction

Increased industrial growth has led to the release of effluents with high amounts of heavy metals, such as mercury, which is one of the most dangerous pollutants that can potentially affect human health (Wang et al., 2004). Owing to their non-biodegradable nature and persistent character in the environment, high concentrations of these ions are a great concern in the scientific community. Research has been conducted to overcome this issue by developing materials and methods to decrease the concentrations of this toxic trace in water (Aguayo-Villarreal et al., 2011), including ion exchangers and adsorbents such as zeolites (Morency, 2002; Theron et al., 2008), biopolymers (Kostal et al., 2001; Shafaei et al., 2007; Zhang et al., 2013), magnetite nanoparticles (Hakami et al., 2012), carbon nanotubes (Saleh, 2015), and dendrimers (Niu et al., 2014).

The methods currently in practice for heavy metal removal include a work by Shahrokhi-Shahraki et al. (2021) in which activated carbon derived from pulverized waste tires exhibited great potential to adsorb three synthetic heavy metal ions: Pb^{2+}, Cu^{2+} and Zn^{2+} from aqueous solution. Results proved that synthesized activated carbon had a monolayer adsorption capacity with faster sorption rate in comparison to commercial activated carbons. Other research work determined the potential of activated carbon collected from a full-scale water treatment plant on removing heavy metals (Dong et al., 2018). By measuring the initial and final concentrations of metals in a batch system, the study found that the activated carbon had a significant adsorption capacity for Pb^{2+} with removal rates above 95% and for Cd^{2+} reporting rates of 86%. This study also provides information on selective adsorption of activated carbon for Pb^{2+} with no reported changes in the surface morphology of the material. These studies highlight the performance of different activated carbon-based materials and the internal structure effects. However, activated carbons as raw materials are usually based in powdery form and require treating with different binders to achieve accurate shape for its applications.

According to a study made by Chen et al. (2022) activated carbon incorporation in geopolymer synthesis developed a composite based on hierarchical pore structures with ultra-micropores and mesopores. The material exhibited an increasing oxygen-containing groups with high activated carbon content, which facilitates CO_2 adsorption capacity and CO_2/N_2 selectivity. Similarly, (Candamano et al., 2022) reported the formulation of geopolymer/NaX/activated carbon foamed composites for CO_2 adsorption/desorption. This study gave an insight about the effect of thermal treatment on the textural properties of the adsorbents and the refining of activated carbon pore size distribution. Obtained materials developed ultra-microporosity and showed high CO_2 storage performance compared with commercial geopolymers.

A recent work by Wang et al. (2022) suggested the use of phosphoric acid-activated geopolymer microspheres with activated carbon for a fast adsorptive separation of ReO4-. This result was successful in obtaining environmentally friendly microspheres with high mechanical properties, proper sphericity, and stable structure, achieving a rapid solid to liquid separation and potential application in column-based separation systems. Although one of the most used materials for heavy metal adsorption is activated carbon, the use of geopolymers based on metakaolin and activated carbon for Hg2 removal has been poorly documented in literature.

Geopolymers are three-dimensional systems with an aluminosilicate frame that were first synthesized by Davidovits in the 1970s (Davidovits, 1991; Davidovits, 1994). These systems, also known in many instances as inorganic polymers, have attracted great attention from academia and industry because of their properties, including thermal stability, chemical and fire resistance, encapsulation of radioactive substances, high durability, low permeability, and high compressive strength (Khale & Chaudhary, 2007; Lyon et al., 1997; Van Jaarsveld et al., 1997; Yunsheng et al., 2010).

The mechanism for producing geopolymers is known as geopolymerization and involves several chemical reactions where the aluminosilicate source is dissolved in a highly alkaline solution, and Al–O and Si–O bonds are released to form sialate groups with tetravalent aluminum and pentavalent silicon atoms. Further condensation reactions promote the formation of ortho-sialate molecules, known as the basic units of geopolymer structures, which react via ionic interactions to form a poly sialate chain. After polycondensation, the final structure consisted of an amorphous to semi-crystalline chain of Si–O–Al bonds in tetrahedral coordination (Davidovits, 2008; Xu & Van Deventer, 2000). Geopolymerization can be performed at room temperature; thus, these materials have a low energy use and, therefore, low emissions of nitrogen oxides (NO_x), sulfur oxides (SO_x), and carbon dioxide (CO_2) (Duxson et al., 2007; Roy, 1999; Shi et al., 2011; Van Deventer et al., 2012; Zhang et al., 2021).

Inorganic polymers can be synthesized from natural aluminosilicate sources into industrial byproducts, such as kaolin, metakaolin, fly ash, red mud, sludge, and rice husk ash (He et al., 2013; Lecomte et al., 2003; Panagiotopoulou et al., 2007). However, the most used source is metakaolin, considering its accessibility, workability, and satisfactory properties compared to those of fly ash and slag-based composites. Metakaolin-based geopolymers have been characterized as porous materials; thus, in the present work, we propose a geopolymer composite that supports activated carbon particles to provide a micro-and mesoporous interface, enhancing the available sites for the leaching of Hg^{2+} ions. These sorbents provide several functional groups that can interact with Hg^{2+} ions via adsorption and ion exchange

mechanisms. Such properties generate a low-cost material that can overcome high temperatures and pressures for industrial applications, solving an environmental problem related to mercury pollution.

2. Materials and methods

2.1. Raw materials

Kaolin clay (KC) used as aluminosilicate source in this study was collected from Michoacan, Mexico. Metakaolin (MK) was prepared by calcining kaolin at 750°C during 3 h using a heating rate of 5°C/min. The obtained metakaolin was passed through No. 200 sieve. Commercial activated carbon (AC) was purchased from CarbUSA LLC, New York. The chemical composition of KC and MK were determined by X-ray fluorescence spectroscopy (Bruker, S2 Ranger spectrometer) measurements used a palladium target. The results are presented in Table 1.

Alkali-silicate solution was prepared by mixing sodium silicate solution (Na_2O = 8.16 wt%, SiO_2 = 26.01 wt%, H_2O = 65.83 wt%) with laboratory grade sodium hydroxide (NaOH, 96% purity) and deionized water. NaOH pellets were completely dissolved under magnetic stirring. Previously, solutions were stored for 24h until reaching equilibrium of the forming species. All reactants were purchased from Sigma Aldrich and used without further purification.

Table 1. Chemical composition of kaolin and metakaolin using the XRF technique.

Composition, wt%	Sample	
	Kaolin (KC)	Metakaolin (MK)
SiO_2	73.5	73.6
Al_2O_3	20.5	21.21
CaO	0.36	0.32
P_2O_5	1.46	1.42
MnO	0.40	0.38
Fe_2O_3	0.19	0.18
SO_3	1.92	1.24
K_2O	0.99	0.96
ZrO_2	0.14	0.14
TiO_2	0.56	0.55

2.2. Synthesis of geopolymer composite

As shown in the scheme displayed in Figure 1 geopolymers (GP) were prepared by mixing metakaolin and alkaline solution with a certain amount of deionized water, using solid-to-liquid (S/L) ratios of 0.5, 0.6 and 0.7. The paste was under mechanical stirring at 400-450 rpm for 5 min to obtain a uniform mixture. After complete homogenization the geopolymer paste was then cast in cylindrical PVC molds of 25.4 x 50.8 mm. All samples were vibrated for 3 min to remove entrapped air bubbles and then tightly wrapped in plastic film to prevent water loss.

The synthesis of geopolymer composite (GP/AC) followed the above process, using MK and AC in proportion of 50:50 wt%/wt%. Both GP and GP/AC were placed in desiccators at room temperature for 24 h before demolding. Finally, samples were heated at 70 °C for 12 h and stored into a desiccator for 7, 14 and 28 days.

2.3. Adsorption of Hg^{2+} ions in aqueous solution

The study of Hg^{2+} removal was carried out using a geopolymer powder dosage of 0.07 g mixed with 50 mL of Hg^{2+} with initial concentration of 100 ppm. The solution was stirred for 300 min at a temperature of 25 °C. Each experiment was repeated at pH values 3, 5 and 7. The amount of metal uptake capacity by geopolymer was obtained according to the mass balance Equation (1), while the removal efficiency of Hg^{2+} ions was calculated using the Equation (2):

$$q = \frac{(C_0 - C_{eq}) \times V}{m} \quad (1)$$

$$Removal\ efficiency\ (\%) = \frac{(C_0 - C_{eq})}{C_0} \times 100 \quad (2)$$

where q is the amount of metal ions uptake (mg Hg^{2+}/g geopolymer); C_0 and C_{eq} are the initial and final concentrations of Hg^{2+} in aqueous solution (mg Hg^{2+}/L), respectively; V is the volume of Hg^{2+} solution (L) and m is the mass of the adsorbent (g).

2.4. Characterization

Chemical structures of geopolymer composites were investigated by Fourier transform infrared spectroscopy (FTIR) using a Perkin Elmer apparatus model Spectrum One in transmission mode. The samples were pressed into KBr pellets (1.5 mg powdered sample mixed with 150 mg KBr). Spectra were recorded at room temperature in the region between 400 cm-1 and 4000 cm-1 using a resolution of 2 cm^{-1}.

Compressive strength was measured using an Instron 1121 universal machine with a load cell for maximum capacity of 300 kN. Following the procedure listed on ASTM C39 (Roy, 1999) three cylindrical specimens with a dimension of 25 mm × 50 mm (diameter × length) were tested after 7, 14 and 28 days of curing at room temperature. Using a crosshead speed of 0.5 mm min^{-1} the load was applied up until failure. Microstructure and morphology were evaluated by a scanning electron microscope (SEM) using a JEOL apparatus model JSM 6390 LV operated at 25 kV.

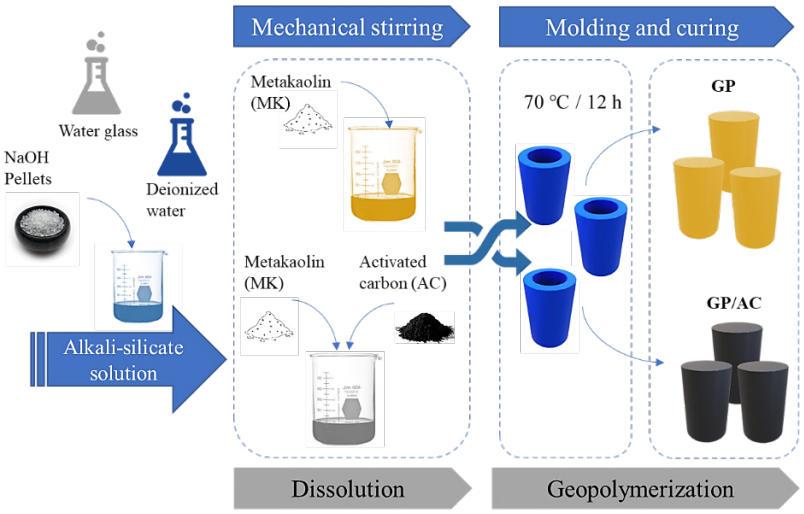

Figure 1. Schematic illustration of synthesis process for GP and GP/AC composites.

Samples were previously coated with a gold layer in a Denton Vacuum Desk IV sputtering system. The concentrations of Hg^{2+} ions were determined by inductively coupled plasma optical emission spectrometer (ICP-OES) using a Perkin Elmer Optimum 2100 DB. Prior to elemental analysis acid digestion was performed following EPA 3015A method, samples were digested using a PerkinElmer Titan MPS microwave.

pH-meter model pH120 Conductronic was used for pH measurements, previously calibrated with a 2-point calibration method using pH 4.0 and 7.0 buffer solutions.

3. Results

The XRD patterns of samples under S/L of 0.7 are shown in Figure 2. As can be seen AC displays one strong broad peak at approximately 2θ = 23.35° which is attributed to interplanar spacing (200), while a weak peak emerged at 2θ = 44.52° attributed to interplanar spacing (100). These results confirmed the existence of graphite crystalline phase (Liu et al., 2014; Zhao et al., 2009). Previous studies have widely reported the mineralogy of KC (Aziz et al., 2021; Dewi et al., 2018; Kumar & Lingfa, 2020), since raw material for the synthesis of geopolymers is metakaolin, the mineralogy for pure MK is detailed. Figure 2 shows that pure MK displayed a hump between the range of 2θ = 15° - 25°, which is characteristic of abundant aluminosilicates with pozzolanic activity (Wang et al., 2005). The pattern also exhibited peaks at 20.81°, 21.91°, 26.66°, 36.04°, 39.57° and 50.17° attributable to quartz and muscovite impurities (Granizo et al., 2007; Zhang et al., 2013).

After alkaline activation of raw materials under thermal treatment, GP synthesized using an S/L ratio of 0.7 displayed a diffuse halo that shifts to higher diffraction angles than MK sample, in the region of 2θ = 20° - 40°. This can be attributed to the geopolymerization reaction of aluminosilicates and therefore, the amorphous structure formed (Masi et al., 2014; Provis et al., 2009; Temuujin et al., 2011). In comparison, GP/AC exhibited a wider dispersed peak in the range of 2θ = 20° - 45° contributed by the AC surface (002) and leads to the formation of a more disordered phase than GP sample.

On the other hand, peaks of quartz detected in MK did not change appreciably under activation and remained in all geopolymer samples. This may be attributed to a low dissolution of crystalline quartz into alkaline solution (Palmero et al., 2015); however, the presence of these peaks does not inhibit polycondensation. The XRD pattern of GP and GP/AC samples also gave an insight about the presence of sodalite peaks in the range of 2θ = 24°-29°. These results agree with previous studies reported in literature (Provis & Van Deventer, 2014; Rattanasak & Chindaprasirt, 2009; Zibouche et al., 2009).

Figure 3 shows the compressive strength of the geopolymer samples at different ages. It was observed that AC tends to decrease compressive strength of geopolymers because of its high porosity. However, it was found that adjusting the solid-to-liquid ratio from 0.5 to 0.7 leads to denser materials and thus, the structure strength of geopolymers was enhanced. From 7 to 14 days of curing at room temperature, all geopolymer samples displayed slightly increased compressive strength. This can be attributed to an incomplete formation of AlO4 and SiO4 oligomers in tetrahedral coordination, during geopolymerization reaction.

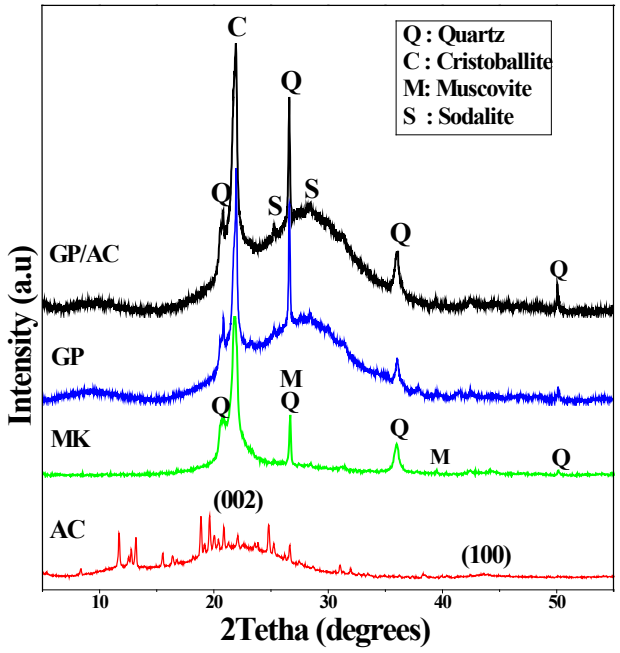

Figure 2. XRD patterns of AC, MK, GP, and GP/AC composites using a S/L of 0.7.

After 28 days of curing, the formation of a more stable network was achieved and the maximum compressive values were observed ranging from 18.73 MPa to 24.31 MPa for GP/AC and GP, respectively. The impact of S/L ratios in the compressive strength of samples is shown in Figure 3, this parameter plays an important role in the mechanical performance of materials under study. Increasing S/L ratio from 0-6 to 0.7 led to higher values of the mechanical property, this can be attributed to the ratio of aluminosilicates in the activator solution.

Previous studies reported that S/L mass ratio affects the compressive strength of geopolymers by interfering with the viscosity of the slurry and geopolymerization set up (Heah et al., 2012; Zuhua et al., 2009), both ratios contribute to the dissolution and polycondensation of species which are important processes during polymerization (Liew et al., 2011; Mert et al., 2019).

For a better understanding of morphology and microstructure, raw materials and geopolymers were investigated by SEM. Their corresponding micrographs are displayed in Figure 4. As can be seen in Figure 4(a) AC has porous particles with a size distribution of 57–171 µm, and a very stable lamellar structure which can facilitate the adsorption of Hg^{2+} ions onto the geopolymer surface.

On the other hand, Figure 4(b) exhibits MK morphology with dominantly plate-like particles of irregular shape, matching with studies previously reported (Fonseca-Páez et al., 2019; Ríos et al., 2009; Youssef et al., 2008).

After alkaline activation the formation of a gel phase is clearly shown in Figure 4(c), suggesting the successful geopolymerization of aluminosilicates. However, unreacted particles were identified on GP, which reveal the existence of crystallites throughout the network. This consists well with the XRD analysis. In the case of GP/AC morphology, a drastic change occurred as observed in Figure 4(d). When activated carbon is added, most of the surface displayed less homogeneity than GP sample. Some irregular cracks can be observed, which are attributed to water evaporation during activation. This provided a reduced compact morphology and therefore, less mechanical resistance compared with GP.

The adsorption capacity of Hg^{2+} ions from aqueous solution using GP and GP/AC was evaluated and the corresponding results are given in Figure 5. In the first 60 minutes high removal occurred as observed in Figure 5a, with a Hg^{2+} uptake ranging from 21.9 to 23.07 mg/g for GP and GP/AC, respectively. Further sorption time showed a clear difference between the adsorbents, at 300 minutes GP/AC reached 27.05 mg/g while GP removed 21.04 mg/g of Hg^{2+} ions. Longer sorption times did not display significant removal and therefore 300 minutes was considered as the equilibrium time for the study.

It should be highlighted that the equilibrium time reported here is smaller compared with some powered and non-powdered materials previously reported (Ma et al., 2009; Sun et al., 2011; Yu et al., 2016). The addition of AC into geopolymer structure has an important effect in adsorption capacity and this could be attributed to the presence of more intense sodalite peaks in GP/AC sample, according to the XRD pattern previously reported in Figure 2. Prior studies reported sodalite as a type of zeolite with a chemical structure of hydrated aluminosilicates forming an arrangement of Al, Si, O and H interconnected in a honeycomb framework (Candamano et al., 2022), the zeolite properties include a high ion-exchange capacity and unique affinity for heavy metal positive ions. Thus, it seems that sodalite crystals in GP/AC sample are increasing the ion-exchange capacity by promoting the presence cavities in negatively charged lattices (Lou et al., 2009). Therefore, the use of geopolymer adsorbents based on metakaolin and activated carbon demonstrate its potential for fast sorption of Hg^{2+} species and further applications associated to mercury pollution.

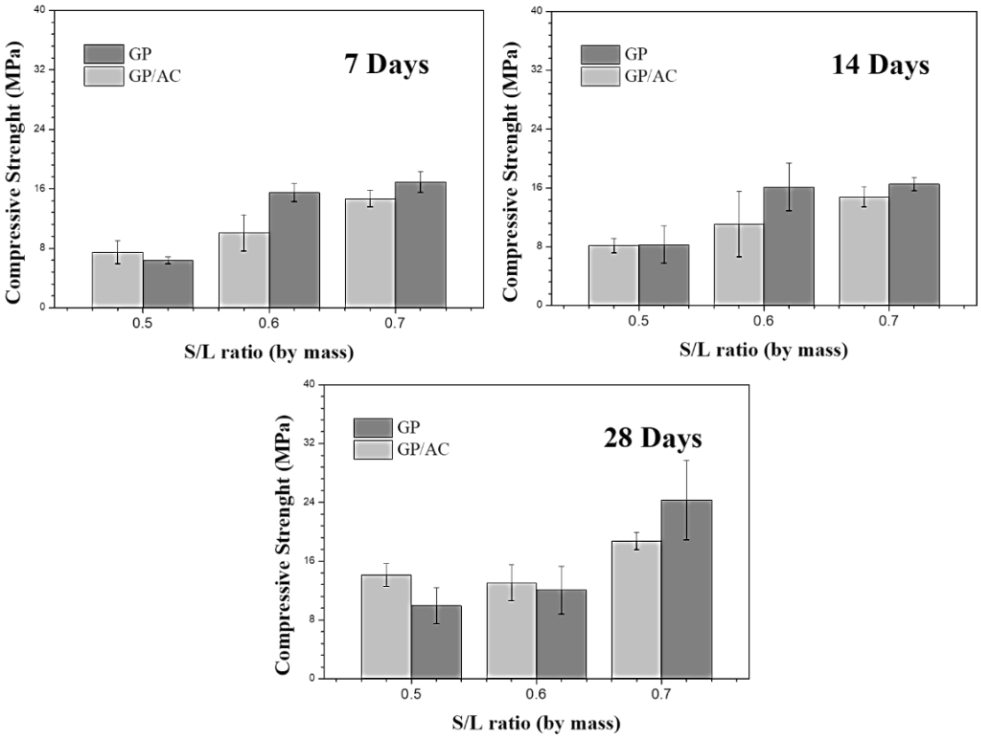

Figure 3. Compressive strength of GP and GP/AC geopolymers as a function of S/L ratios.

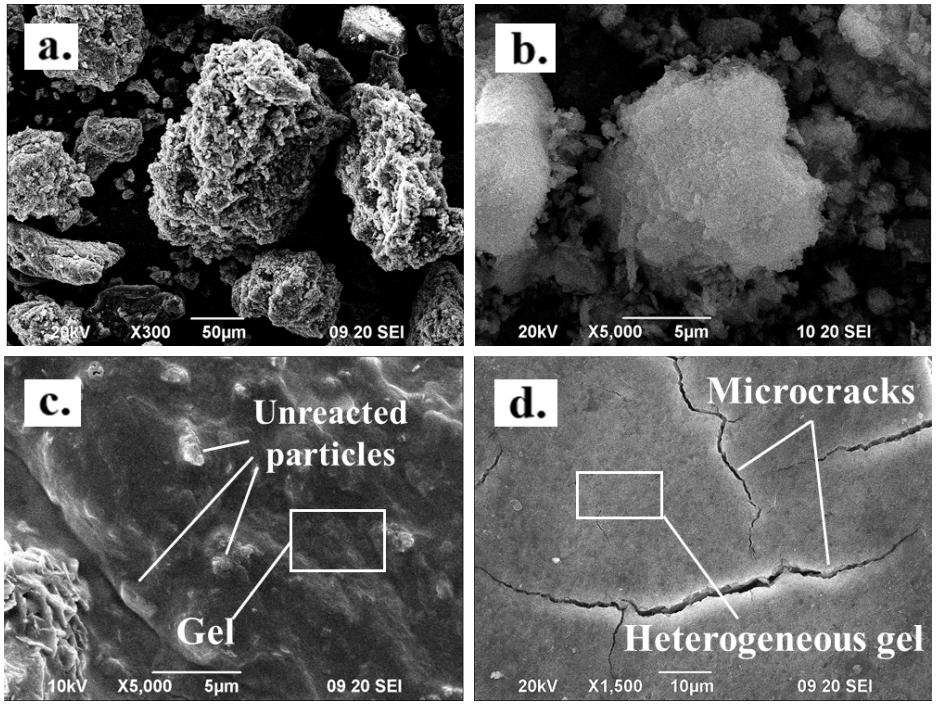

Figure 4. SEM micrographs of a) AC, b) MK, c) GP and d) GP/AC.

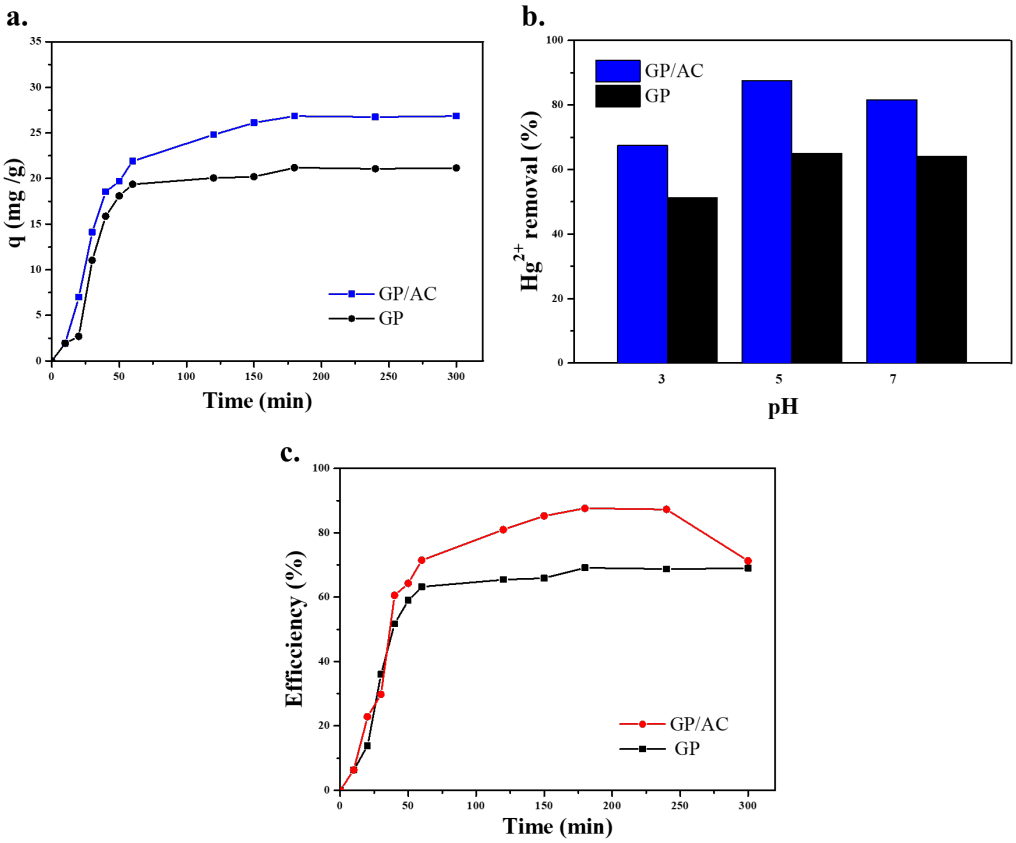

Figure 5. a) Adsorption kinetics of GP and GP/AC b) Effect of pH on the adsorption of Hg^{2+} ions and c) Removal efficiency of GP and GP/AC.

Figure 5b exhibits that pH is an important parameter that significantly affects the removal efficiency of Hg^{2+} ions. It was found that an increase in solution pH from 3 to 5 led to an increase in removal efficiency from 51.2 % to 65 % in GP samples. Similarly, GP/AC samples reported an increase of 67.4 % to 87.6 %. At pH 7 a slight decrease was observed in both sorbents, reporting efficiencies of 64.2 % and 81.6 % for GP and GP/AC, respectively. This result suggests the different species formed according to pH values, in which below pH 5 the main species acquire negative charge causing repulsions and less efficient uptake of Hg^{2+} ions. The effect of contact time on removal efficiency is depicted in Figure 5c. After 60 min 63.1 % of removal is reached for GP and 71.5 % for GP/AC. After 180 min of contact time, the efficiency increased slowly and achieved the maximum removal with 69.2 % for GP and 87.6 % for GP/AC. This result implies that initially the sorbents possess abundantly active sites, which progressively are occupied by different species, over time the number of active sites decrease as well as free alkalis available for leaching. Consequently, a decrease in adhesion forces is created between the surface and Hg^{2+} ions, reducing the removal efficiency after longer periods of time. The removal efficiency and adsorption capacities of Hg^{2+} ions from previous studies were lower than those achieved by the present study (Gupta et al., 2004; Machida et al., 2004; Machida et al., 2005; Rong et al., 2018; Zou et al., 2018).

Figure 6 shows FTIR spectrum before and after the adsorption test. As can be seen all samples exhibited peaks between 3435 cm-1 and 3328 cm-1 which are attributed to –OH stretching and bending vibrations. Figure 6a display recorded for GP sample before adsorption test, it is noted two bands at about 1462 cm-1 and 1390 cm-1 which are attributed to the presence of stretching vibration of the O–C–O bonds. This group can be related to the reaction of sodium hydroxide with atmospheric CO_2 during geopolymerization (Chindaprasirt et al., 2009) forming Na_2CO_3.

The appearance of peaks at 872 cm-1 and 848 cm-1 verified the bonding of Al–O tetrahedral. After adsorption, a significant difference is observed with O-C-O and Al-O groups as observed in Figure 6b, intensity of the bands almost disappeared. This indicates the interactions between both groups with Hg^{2+} ions. In the case of GP/AC spectra displayed in Figure 6c before adsorption a characteristic peak at 1460 cm-1 is observed. This band is assigned to the stretching vibrations of C=O related to

carboxylic and carboxylate groups. A peak at 851 cm-1 is also observed, revealing the presence of A–O groups in the sample. After adsorption, a decrease in intensity of these bands is clearly shown in Figure 6d. Modification of intensities verified the involvement of these groups during metal removal and revealed the coordination with Hg^{2+} ions onto the surface of the sorbents proposed.

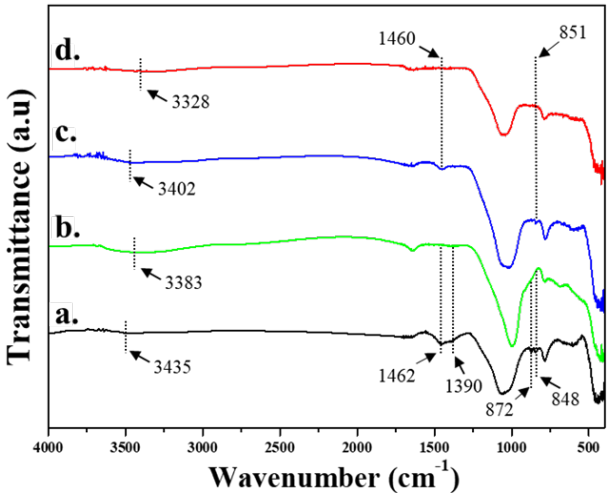

Figure 6. FTIR spectra of all samples before and after adsorption of Hg^{2+} ions. a) GP, b) GP after removal, c) GP/AC and d) GP/AC after removal.

4. Conclusions

In this work, a metakaolin-based geopolymer containing activated carbon was developed. The composite exhibits the maximum compressive strength at 28 days of curing, and increases from 8.1 to 18.73 MPa, when the S/L ratio is fixed from 0.5 to 0.7. The optimum pH for the maximum adsorption of Hg^{2+} ions is found to be pH: 5, with initial concentration of 100 ppm, agitation time of 300 min and sorbent dosage of 0.07 g. The addition of activated carbon improved the removal efficiency from 65% to 87.6 %. According to FTIR analysis the adsorption is strongly affected by coordination of carboxylic, carboxylate and Al-O groups with Hg^{2+} ions. These results show that activated carbon successfully improved the adsorption capacity of metakaolin-based geopolymers, suggesting the possibility of using the porous composite for further applications linked to mercury removal.

Conflict of interest

The authors do not have any type of conflict of interest to declare.

Funding

This research was funded by Pedagogical and Technological University of Colombia –UPTC. It was also supported by the Center for Research in Applied Science and Advanced Technology (CICATA) from the National Polytechnic Institute National Polytechnic Institute (IPN) – Mexico.

References

Aguayo-Villarreal, I. A., Bonilla-Petriciolet, A., Hernández-Montoya, V., Montes-Morán, M. A., & Reynel-Avila, H. E. (2011). Batch and column studies of Zn2+ removal from aqueous solution using chicken feathers as sorbents. *Chemical Engineering Journal, 167*(1), 67–76. https://doi.org/10.1016/j.cej.2010.11.107

ASTM C39/C39M. Standard test method for compressive strength of cylindrical concrete specimens. American Society for Testing and Materials, Philadelphia, 2002.

Aziz, A., Bellil, A., El Hassani, I. E. E. A., Fekhaoui, M., Achab, M., Dahrouch, A., & Benzaouak, A. (2021). Geopolymers based on natural perlite and kaolinic clay from Morocco: Synthesis, characterization, properties, and applications. *Ceramics International*, *47*(17), 24683-24692. https://doi.org/10.1016/j.ceramint.2021.05.190

Shi, C., Jiménez, A. F., & Palomo, A. (2011). New cements for the 21st century: The pursuit of an alternative to Portland cement. *Cement and concrete research*, *41*(7), 750-763. https://doi.org/10.1016/j.cemconres.2011.03.016

Candamano, S., Policicchio, A., Conte, G., Abarca, R., Algieri, C., Chakraborty, S., ... & Agostino, R. G. (2022). Preparation of foamed and unfoamed geopolymer/NaX zeolite/activated carbon composites for CO2 adsorption. *Journal of Cleaner Production*, *330*, 129843. https://doi.org/10.1016/j.jclepro.2021.129843

Chen, H., Liu, L. C., Dong, S., Zhang, Y., & He, P. (2022). Development of a new type of phosphoric acid based geopolymer/activated carbon composite for selective CO2 capture. *Materials Letters*, *325*, 132869. https://doi.org/10.1016/j.matlet.2022.132869

Chindaprasirt, P., Jaturapitakkul, C., Chalee, W., & Rattanasak, U. (2009). Comparative study on the characteristics of fly ash and bottom ash geopolymers. *Waste Management, 29*(2), 539–543. https://doi.org/10.1016/j.wasman.2008.06.023

Davidovits, J. (1991). Geopolymers: inorganic polymeric new materials. *Journal of Thermal Analysis and calorimetry*, *37*(8), 1633-1656. https://doi.org/10.1007/BF01912193

Davidovits, J. (1994). Properties of geopolymer cements. In First international conference on alkaline cements and concretes (Vol. 1, pp. 131-149).

Davidovits, J. (2008). Geopolymer Chemistry and Applications. Geopolymer Institute, Saint-Quentin, France. ISBN 2-951-14820-1-9.

Dewi, R., Agusnar, H., Alfian, Z., & Tamrin. (2018). Characterization of technical kaolin using XRF, SEM, XRD, FTIR and its potentials as industrial raw materials. In *Journal of Physics: Conference Series* (Vol. 1116, p. 042010). IOP Publishing. https://doi.org/10.1088/1742-6596/1116/4/042010

Dong, L., Hou, L. A., Wang, Z., Gu, P., Chen, G., & Jiang, R. (2018). A new function of spent activated carbon in BAC process: Removing heavy metals by ion exchange mechanism. *Journal of Hazardous Materials*, *359*, 76-84. https://doi.org/10.1016/j.jhazmat.2018.07.030

Duxson, P., Fernández-Jiménez, A., Provis, J. L., Lukey, G. C., Palomo, A., & van Deventer, J. S. (2007). Geopolymer technology: the current state of the art. *Journal of materials science*, *42*, 2917-2933. https://doi.org/10.1007/s10853-006-0637-z

Fonseca-Páez, L. A., Roa-Bohórquez, K. L., Vera-López, E., & Peña-Rodríguez, G. (2019). Microstructure, physical and mechanical properties of kaolin-diatomite composite reinforced with CaCO3. *DYNA*, *86*(210), 323-332. http://doi.org/10.15446/dyna.v86n210.77450

Granizo, M. L., Blanco-Varela, M. T., & Martínez-Ramírez, S. (2007). Alkali activation of metakaolins: Parameters affecting mechanical, structural and microstructural properties. *Journal of Materials Science, 42*(9), 2934–2943. https://doi.org/10.1007/s10853-006-0565-y

Gupta, V. K., Singh, P., & Rahman, N. (2004). Adsorption behavior of Hg (II), Pb (II), and Cd (II) from aqueous solution on Duolite C-433: a synthetic resin. *Journal of Colloid and Interface Science*, *275*(2), 398-402. https://doi.org/10.1016/j.jcis.2004.02.046

Hakami, O., Zhang, Y., & Banks, C. J. (2012). Thiol-functionalised mesoporous silica-coated magnetite nanoparticles for high efficiency removal and recovery of Hg from water. *Water Research, 46*(12), 3913–3922. https://doi.org/10.1016/j.watres.2012.04.032

He, J., Jie, Y., Zhang, J., Yu, Y., & Zhang, G. (2013). Synthesis and characterization of red mud and rice husk ash-based geopolymer composites. *Cement and Concrete Composites*, *37*, 108-118. https://doi.org/10.1016/j.cemconcomp.2012.11.010

Heah, C. Y., Kamarudin, H., Al Bakri, A. M., Bnhussain, M., Luqman, M., Nizar, I. K., ... & Liew, Y. M. (2012). Study on solids-to-liquid and alkaline activator ratios on kaolin-based geopolymers. *Construction and Building Materials*, *35*, 912-922. https://doi.org/10.1016/j.conbuildmat.2012.04.102

Khale, D., & Chaudhary, R. (2007). Mechanism of geopolymerization and factors influencing its development: a review. *Journal of materials science*, *42*, 729-746. https://doi.org/10.1007/s10853-006-0401-4

Kostal, J., Mulchandani, A., & Chen, W. (2001). Tunable biopolymers for heavy metal removal. *Macromolecules, 34*(7), 2257–2261. https://doi.org/10.1021/ma001973m

Kumar, A., & Lingfa, P. (2020). Sodium bentonite and kaolin clays: Comparative study on their FT-IR, XRF, and Xrd. *Materials Today: Proceedings*, 22, 737-742. https://doi.org/10.1016/j.matpr.2019.10.037

Lecomte, I., Liégeois, M., Rulmont, A., Cloots, R., & Maseri, F. (2003). Synthesis and characterization of new inorganic polymeric composites based on kaolin or white clay and on ground-granulated blast furnace slag. *Journal of materials research*, *18*(11), 2571-2579. https://doi.org/10.1557/JMR.2003.0360

Liew, Y. M., Kamarudin, H., Bakri, A. M. M., Binhussain, M., Luqman, M., Nizar, I. K., Ruzaidi, C. M., & Heah, C. Y. (2011). Influence of solids-to-liquid and activator ratios on calcined Kaolin Cement Powder. *Physics Procedia*, *22*, 312–317. https://doi.org/10.1016/j.phpro.2011.11.049

Liu, D., Yuan, W., Deng, L., Yu, W., Sun, H., & Yuan, P. (2014). Preparation of porous diatomite-templated carbons with large adsorption capacity and mesoporous zeolite K-H as a byproduct. *Journal of Colloid and Interface Science, 424*, 22–26. https://doi.org/10.1016/j.jcis.2014.03.001

Lou, J. C., Chang, T. W., & Huang, C. E. (2009). Effective removal of disinfection by-products and assimilable organic carbon: An advanced water treatment system. *Journal of Hazardous Materials*, *172*(2-3), 1365-1371. https://doi.org/10.1016/j.jhazmat.2009.07.151

Lyon, R. E., Balaguru, P. N., Foden, A., Sorathia, U., Davidovits, J., & Davidovics, M. (1997). Fire-resistant aluminosilicate composites. *Fire and materials*, *21*(2), 67-73. https://doi.org/10.1002/(SICI)1099-1018(199703)21:2<67::AID-FAM596>3.0.CO;2-N

Ma, F., Qu, R., Sun, C., Wang, C., Ji, C., Zhang, Y., & Yin, P. (2009). Adsorption behaviors of Hg (II) on chitosan functionalized by amino-terminated hyperbranched polyamidoamine polymers. *Journal of hazardous materials*, *172*(2-3), 792-801. https://doi.org/10.1016/j.jhazmat.2009.07.066

Machida, M., Aikawa, M., & Tatsumoto, H. (2005). Prediction of simultaneous adsorption of Cu (II) and Pb (II) onto activated carbon by conventional Langmuir type equations. *Journal of Hazardous materials*, *120*(1-3), 271-275. https://doi.org/10.1016/j.jhazmat.2004.11.029

Machida, M., Kikuchi, Y., Aikawa, M., & Tatsumoto, H. (2004). Kinetics of adsorption and desorption of Pb (II) in aqueous solution on activated carbon by two-site adsorption model. *Colloids and Surfaces A: Physicochemical and Engineering Aspects*, *240*(1-3), 179-186. https://doi.org/10.1016/j.colsurfa.2004.04.046

Masi, G., Rickard, W. D. A., Vickers, L., Bignozzi, M. C., & Van Riessen, A. (2014). A comparison between different foaming methods for the synthesis of light weight geopolymers. *Ceramics International, 40*(9), 13891–13902. https://doi.org/10.1016/j.ceramint.2014.05.108

Mert, M. S., Mert, H. H., & Sert, M. (2019). Investigation of thermal energy storage properties of a microencapsulated phase change material using response surface experimental design methodology. *Applied Thermal Engineering*, *149*, 401-413. https://doi.org/10.1016/j.applthermaleng.2018.12.064

Morency, J. (2002). Zeolite sorbent that effectively removes mercury from flue gases. *Filtration and Separation, 39*(7), 24–26. https://doi.org/10.1016/S0015-1882(02)80207-5

Niu, Y., Qu, R., Chen, H., Mu, L., Liu, X., Wang, T., Zhang, Y., & Sun, C. (2014). Synthesis of silica gel supported salicylaldehyde modified PAMAM dendrimers for the effective removal of Hg(II) from aqueous solution. *Journal of Hazardous Materials, 278*, 267–278. https://doi.org/10.1016/j.jhazmat.2014.06.012

Palmero, P., Formia, A., Antonaci, P., Brini, S., & Tulliani, J. M. (2015). Geopolymer technology for application-oriented dense and lightened materials. Elaboration and characterization. *Ceramics International, 41*(10), 12967–12979. https://doi.org/10.1016/j.ceramint.2015.06.140

Panagiotopoulou, C., Kontori, E., Perraki, T., & Kakali, G. (2007). Dissolution of aluminosilicate minerals and by-products in alkaline media. *Journal of Materials Science*, *42*, 2967-2973. https://doi.org/10.1007/s10853-006-0531-8

Provis, J. L., & Van Deventer, J. S. (Eds.). (2013). Alkali activated materials: state-of-the-art report, RILEM TC 224-AAM (Vol. 13). Springer Science & Business Media.

Provis, J. L., Yong, S. L., & Duxson, P. (2009). Nanostructure/microstructure of metakaolin geopolymers. In *Geopolymers* (pp. 72-88). Woodhead Publishing. https://doi.org/10.1533/9781845696382.1.72

Rattanasak, U., & Chindaprasirt, P. (2009). Influence of NaOH solution on the synthesis of fly ash geopolymer. *Minerals Engineering, 22*(12), 1073-1078. https://doi.org/10.1016/j.mineng.2009.03.022

Rios, C. A., Williams, C. D., & Fullen, M. A. (2009). Nucleation and growth history of zeolite LTA synthesized from kaolinite by two different methods. *Applied Clay Science*, *42*(3-4), 446-454. https://doi.org/10.1016/j.clay.2008.05.006

Rong, L., Zhu, Z., Wang, B., Mao, Z., Xu, H., Zhang, L., Zhong, Y., & Sui, X. (2018). Facile fabrication of thiol-modified cellulose sponges for adsorption of Hg 2+ from aqueous solutions. *Cellulose*, 25, 3025-3035. https://doi.org/10.1007/s10570-018-1758-7

Roy, D. M. (1999). Alkali-activated cements opportunities and challenges. *Cement and concrete research*, 29(2), 249-254. https://doi.org/10.1016/S0008-8846(98)00093-3

Saleh, T. A. (2015). Isotherm, kinetic, and thermodynamic studies on Hg(II) adsorption from aqueous solution by silica-multiwall carbon nanotubes. *Environmental Science and Pollution Research, 22*(21), 16721–16731. https://doi.org/10.1007/s11356-015-4866-z

Shafaei, A., Ashtiani, F. Z., & Kaghazchi, T. (2007). Equilibrium studies of the sorption of Hg(II) ions onto chitosan. *Chemical Engineering Journal, 133*(1–3), 311–316. https://doi.org/10.1016/j.cej.2007.02.016

Shahrokhi-Shahraki, R., Benally, C., El-Din, M. G., & Park, J. (2021). High efficiency removal of heavy metals using tire-derived activated carbon vs commercial activated carbon: Insights into the adsorption mechanisms. *Chemosphere*, 264, 128455. https://doi.org/10.1016/j.chemosphere.2020.128455

Sun, C., Ma, F., Zhang, G., Qu, R., & Zhang, Y. (2011). Removal of mercury ions from ethanol solution using silica gel functionalized with amino-terminated dendrimer-like polyamidoamine polymers: Kinetics and equilibrium studies. *Journal of Chemical and Engineering Data, 56*(12), 4407–4415. https://doi.org/10.1021/je200235j

Temuujin, J., Rickard, W., Lee, M., & Van Riessen, A. (2011). Preparation and thermal properties of fire resistant metakaolin-based geopolymer-type coatings. *Journal of Non-Crystalline Solids, 357*(5), 1399–1404. https://doi.org/10.1016/j.jnoncrysol.2010.09.063

Theron, J., Walker, J. A., & Cloete, T. E. (2008). Nanotechnology and Water Treatment: Applications and Emerging Opportunities. *Critical Reviews in Microbiology, 34*(1), 43–69. https://doi.org/10.1080/10408410701710442

Van Deventer, J. S., Provis, J. L., & Duxson, P. (2012). Technical and commercial progress in the adoption of geopolymer cement. *Minerals Engineering*, *29*, 89-104. https://doi.org/10.1016/j.mineng.2011.09.009

Van Jaarsveld, J. G. S., Van Deventer, J. S. J., & Lorenzen, L. (1997). The potential use of geopolymeric materials to immobilise toxic metals: Part I. Theory and applications. *Minerals engineering*, *10*(7), 659-669. https://doi.org/10.1016/S0892-6875(97)00046-0

Wang, H., Li, H., & Yan, F. (2005). Synthesis and mechanical properties of metakaolinite-based geopolymer. *Colloids and Surfaces A: Physicochemical and Engineering Aspects, 268*(1–3), 1–6. https://doi.org/10.1016/j.colsurfa.2005.01.016

Wang, K., Chen, S., Qiu, R., Muhammad, Y., Shao, L., Li, X., ... & Fujita, T. (2022). Convenient preparation of activated carbon modified phosphoric acid-activated geopolymer microspheres (C@ PAAGMs) for the efficient adsorption of ReO4−: implications for TcO4− elimination. *Composites Part B: Engineering*, *247*, 110296. https://doi.org/10.1016/j.compositesb.2022.110296

Wang, Q., Kim, D., Dionysiou, D. D., Sorial, G. A., & Timberlake, D. (2004). Sources and remediation for mercury contamination in aquatic systems - A literature review. *Environmental Pollution*, *131*(2), 323–336. https://doi.org/10.1016/j.envpol.2004.01.010

Xu, H., & Van Deventer, J. S. J. (2000). The geopolymerisation of alumino-silicate minerals. *International journal of mineral processing*, *59*(3), 247-266. https://doi.org/10.1016/S0301-7516(99)00074-5

Youssef, H., Ibrahim, D., & Komarneni, S. (2008). Microwave-assisted versus conventional synthesis of zeolite A from metakaolinite. *Microporous and Mesoporous Materials, 115*(3), 527–534. https://doi.org/10.1016/j.micromeso.2008.02.030

Yu, J. G., Yue, B. Y., Wu, X. W., Liu, Q., Jiao, F. P., Jiang, X. Y., & Chen, X. Q. (2016). Removal of mercury by adsorption: a review. *Environmental Science and Pollution Research*, *23*, 5056-5076. https://doi.org/10.1007/s11356-015-5880-x

Yunsheng, Z., Wei, S., & Zongjin, L. (2010). Composition design and microstructural characterization of calcined kaolin-based geopolymer cement. *Applied Clay Science*, *47*(3-4), 271-275. https://doi.org/10.1016/j.clay.2009.11.002

Zhang, M., Guo, H., El-Korchi, T., Zhang, G., & Tao, M. (2013). Experimental feasibility study of geopolymer as the next-generation soil stabilizer. *Construction and Building Materials, 47*, 1468-1478. https://doi.org/10.1016/j.conbuildmat.2013.06.017

Zhang, Z., Wang, T., Zhang, H., Liu, Y., & Xing, B. (2021). Adsorption of Pb(II) and Cd(II) by magnetic activated carbon and its mechanism. *Science of the Total Environment*, 757, 143910. https://doi.org/10.1016/j.scitotenv.2020.143910

Zhao, J., Yang, L., Li, F., Yu, R., & Jin, C. (2009). Structural evolution in the graphitization process of activated carbon by high-pressure sintering. *Carbon, 47*(3), 744–751. https://doi.org/10.1016/j.carbon.2008.11.006

Zibouche, F., Kerdjoudj, H., de Lacaillerie, J. B. D. E., & Van Damme, H. (2009). Geopolymers from Algerian metakaolin. Influence of secondary minerals. *Applied Clay Science*, *43*(3-4), 453-458. https://doi.org/10.1016/j.clay.2008.11.001

Zou, C., Liang, J., Jiang, W., Guan, Y., & Zhang, Y. (2018). Adsorption behavior of magnetic bentonite for removing Hg (II) from aqueous solutions. *RSC advances*, *8*(48), 27587-27595. https://doi.org/10.1039/C8RA05247F

Zuhua, Z., Xiao, Y., Huajun, Z., & Yue, C. (2009). Role of water in the synthesis of calcined kaolin-based geopolymer. *Applied Clay Science*, *43*(2), 218–223. https://doi.org/10.1016/j.clay.2008.09.003